

PIN OR NEEDLE FRAGMENT HR-3031 - TIN BRONZE - LATE BRONZE AGE - SWITZERLAND

Artefact name	Pin or needle fragment HR-3031
Authors	Marianne. Senn (EMPA, Dübendorf, Zurich, Switzerland) & Christian. Degriigny (HE-Arc CR, Neuchâtel, Neuchâtel, Switzerland)
Url	/artefacts/216/

✖ The object



Credit HE-Arc CR.

Fig. 1: Tin bronze pin or needle fragment (after Rychner-Faraggi 1993, plate 74.11),

✖ Description and visual observation

Description of the artefact	Pin or needle fragment. The patina is green-blue and granulated, typical of terrestrial context. Dimensions: L = 9cm; Ø = 2.5-2.9mm; WT = 3.6g.
Type of artefact	Pin
Origin	Hauterive - Champréveyres, Neuchâtel, Neuchâtel, Switzerland
Recovering date	Excavation 1983-1985, object from layer 1 (layer with material from Bronze Age till 20th cent.)
Chronology category	Late Bronze Age
chronology tpq	<input type="text" value="1050"/> B.C. ▼
chronology taq	<input type="text" value="800"/> B.C. ▼
Chronology comment	Hallstatt A2/B (1050BC _ 800BC)
Burial conditions / environment	Lake
Artefact location	Laténium, Neuchâtel, Neuchâtel
Owner	Laténium, Neuchâtel, Neuchâtel
Inv. number	Hr 3031
Recorded conservation data	Not conserved

✖ Study area(s)



Credit HE-Arc CR.

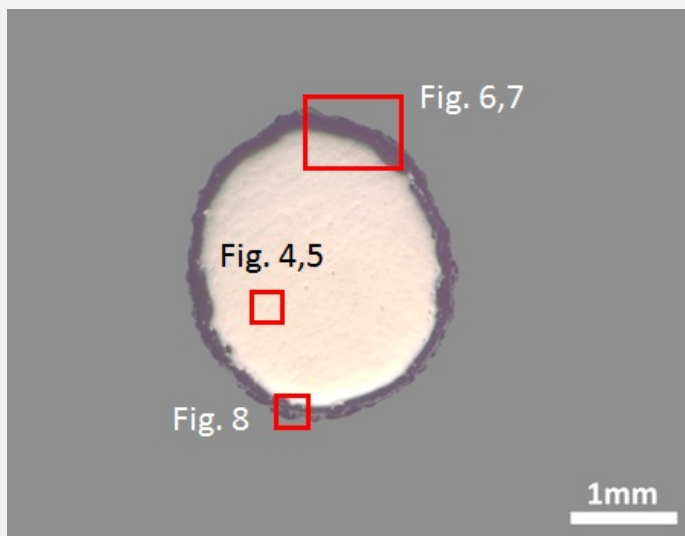
Fig. 2: Location of sampling area,

✧ Binocular observation and representation of the corrosion structure

Stratigraphic representation: none

✧ MiCorr stratigraphy(ies) – Bi

✧ Sample(s)



Credit HE-Arc CR.

Fig. 3: Micrograph of the cross-section showing the locations of Figures 4 to 8,

Description of sample	The cross-section is circular and is a complete section through the pin. The surface is completely covered with a rather thin corrosion crust of irregular thickness.
Alloy	Tin Bronze
Technology	Cold worked after annealing
Lab number of sample	MAH 87-195
Sample location	Musées d'art et d'histoire, Genève, Geneva
Responsible institution	Musées d'art et d'histoire, Genève, Geneva
Date and aim of sampling	1987, metallography and corrosion characterisation

✧ Analyses and results

Analyses performed:

Metallography (etched with ferric chloride reagent), Vickers hardness testing, ICP-OES, SEM/EDX, XRD.

Non invasive analysis

Metal

The remaining metal is a tin bronze and contains small copper sulphide and Pb-rich inclusions evenly distributed throughout the metal (Fig. 4, Tables 1 and 2). The Pb-rich inclusions are only visible with SEM appearing as white particles. The etched structure of the tin bronze shows re-crystallised and angular grains, some of them with twins (Fig. 5). Strain or slip lines are visible, especially near the metal surface. They indicate a final cold working. Copper sulphide inclusions are found both at the grain boundaries and inside the grains (Fig. 5). The average hardness of the metal is about HV1 120.

Elements	Cu	Sn	Sb	Ni	As	Pb	Ag	Co	Zn	Fe
mass%	91.29	5.65	1.00	0.69	0.55	0.51	0.22	0.06	0.01	0.02

Table 1: Chemical composition of the metal. Method of analysis: ICP-OES, Laboratory of Analytical Chemistry, Empa.

Elements	S	Cu	Total
mass%	21	85	106

Table 2: Chemical composition of grey inclusions (Fig. 4). Method of analysis: SEM/EDX, Laboratory of Analytical Chemistry, Empa.

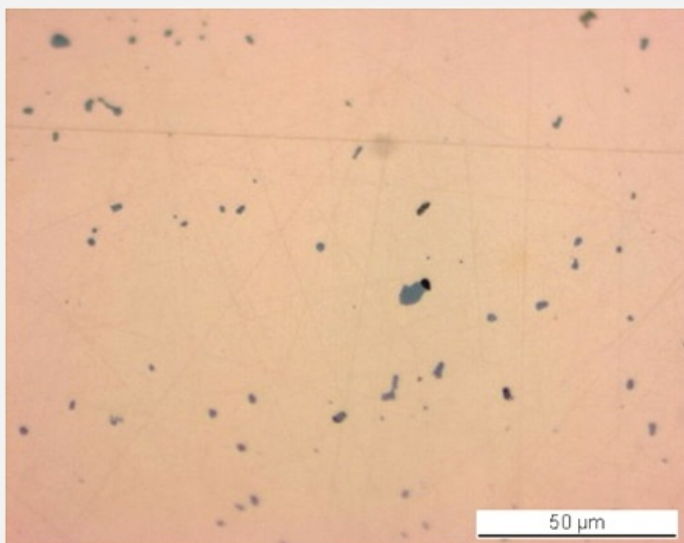


Fig. 4: Micrograph of the metal sample from Fig. 3 (detail), unetched, bright field. Grey copper sulphide inclusions are clearly visible,

Credit HE-Arc CR.

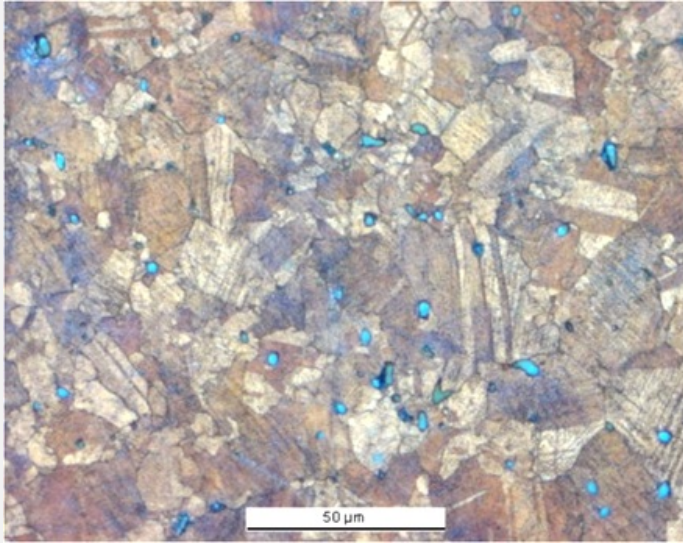


Fig. 5: Micrograph of the metal sample from Fig. 3 (detail), etched, bright field. Small angular re-crystallised grains (some with twins) with slip lines are observed. Copper sulphide inclusions appear in blue,

Credit HE-Arc CR.

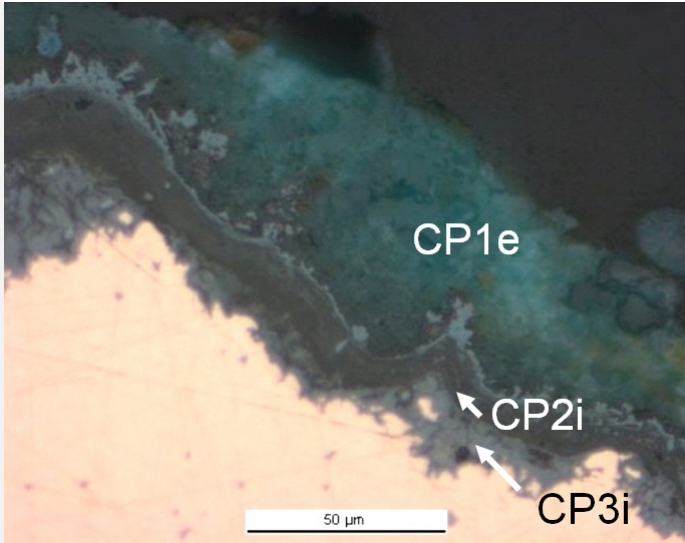
Microstructure	Polygonal and twinned grains + strain lines (metal surface)
First metal element	Cu
Other metal elements	Sn, Sb

Corrosion layers

The corrosion crust has an average thickness of about 50µm (Fig. 6). In polarised light (Fig. 7), the corrosion stratigraphy is more clearly visible: it is composed of an inner orange-red corrosion layer (an agglomerate of nanoscale stannic oxides with cuprite) directly on the metal core (Table 3 and Fig. 8, already studied by Piccardo et al. 2007), an intermediate multi-layered black band and an outer turquoise-green layer analysed with XRD by Schweizer as malachite/CuCO₃Cu(OH)₂ (Schweizer 1994, 150). In some areas the orange-red layers can also be found in between the black band and the malachite. Elemental chemical distribution of the SEM image of Fig. 8 shows that the black layers are enriched in Sn but also contain Fe (Fig. 8). Superior markers such as contextual Al and Si are present in the outer malachite layers. S is present both on the rim of the outer black layer and in the malachite (Fig. 8, Table 3).

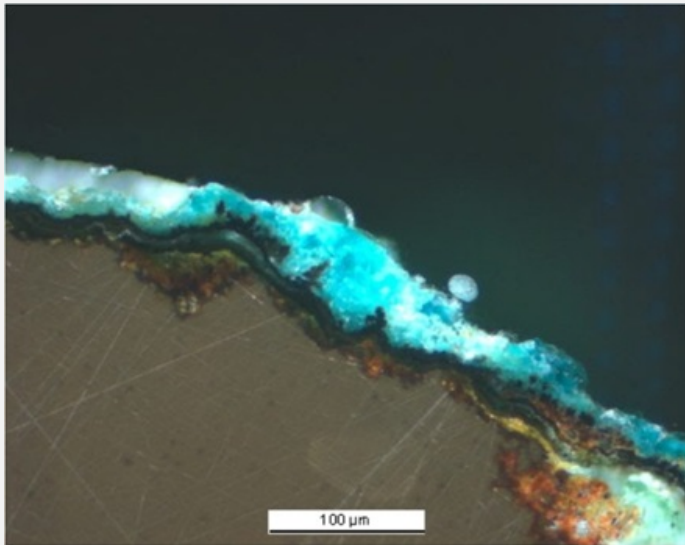
Elements	O	Cu	Sn	S	Cl	Fe	As	Ag	Total
CP3i ext.	20	40	12	15	<	5	<	1.9	94
CP3i int.	20	53	16	<	0.9	<	0.6	<	91

Table 3: Chemical composition (mass %) of orange corrosion products (from Figs. 6 and 7). Method of analysis: SEM/EDX, Laboratory of Analytical Chemistry, Empa.



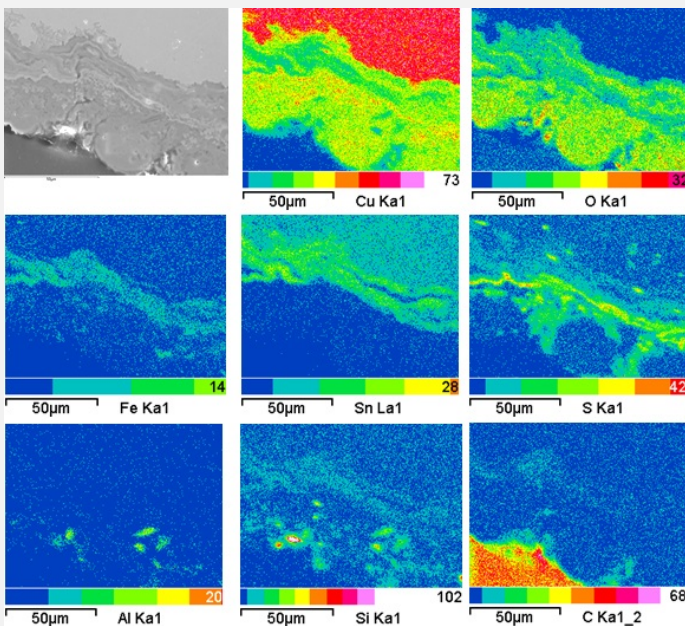
Credit HE-Arc CR.

Fig. 6: Micrograph of the metal sample from Fig. 3 (detail), unetched, bright field. Stratigraphy of the corrosion crust: inner light-grey layer, intermediate dark-grey layer with a light-grey rim and outer grey-green layer,



Credit HE-Arc CR.

Fig. 7: Micrograph of the metal sample from Fig. 3, polarised light. The metal appears in brown; the inner layer appears as red-orange, the intermediate layer as black and the outer layer as turquoise,



Credit HE-Arc CR.

Fig. 8: SEM image, SE-mode, and elemental chemical distribution of a selected area of Fig. 3. Method of examination: SEM/EDX, Laboratory of Analytical Chemistry, Empa,

Corrosion form Multiform - pitting
 Corrosion type Type II (Robbiola)

✚ MiCorr stratigraphy(ies) – CS

Fig. 4: Stratigraphic representation of the object in cross-section using the MiCorr application. This representation can be compared to Figs. 7 and 8.

✚ Synthesis of the binocular / cross-section examination of the corrosion structure

Corrected stratigraphic representation: none

✚ Conclusion

The pin is made from a tin bronze and has been repeatedly cold worked and annealed. After the last annealing there has been some cold work, as can be seen from the strain lines visible after etching the metal. Due to the presence in the corrosion crust of an outer malachite layer, the corrosion was described as terrestrial by Schweizer (Schweizer 1994). The elemental chemical distribution of the corrosion crust shows a more complex situation: as expected for an object buried in a terrestrial site, a typical enrichment of Sn is observed in the inner and intermediate layers covering the surviving metal surface. However it is combined with Fe and S which are often present in lake patinas. According to Schweizer, these layers were formed in anaerobic conditions and developed later on into malachite in an aerated soil through partial dehydration (Schweizer 1994, Schwartz 1934). Since the original surface is absent (destroyed), we refer to type 2 corrosion after Robbiola et al. 1998.

✚ References

References on object and sample

References object

1. Rychner-Faraggi A-M. (1993) Hauterive – Champréveyres 9. Métal et parure au Bronze final. Archéologie neuchâteloise, 17 (Neuchâtel), planche 74.11.

References sample

2. Empa Report 137 695/1991, P.O. Boll.
3. Rapport d'examen, Laboratoire Musées d'art et d'Histoire, Geneva GE (1987), 87-194 à 197.
4. Schwartz, G.M. (1934) Paragenesis of oxidised ores of copper, Economic Geology, 29, 55-75.
5. Schweizer, F. (1994) Objets en bronze provenant de sites lacustres: de leur patine à leur biographie. In: L'œuvre d'art sous le regard des sciences (éd. Rinuy, A. and Schweizer, F.), 143-157.

References on analytic methods and interpretation

6. Interpretation of orange corrosion products, see: Piccardo P., Mille B., Robbiola L. Tin and copper oxide in corroded archaeological bronzes, In: Corrosion of metallic heritage artefacts, European Federation of Corrosion Publication n°48, 2007, ed. Dillmann et al, 239-262.
7. Robbiola, L., Blengino, J-M., Fiaud, C. (1998) Morphology and mechanisms of formation of natural patinas on archaeological Cu-Sn alloys, Corrosion Science, 40, 12, 2083-2111.